Efficient Scheme for Chemical Flooding Simulation

Benjamin Braconnier, Eric Flauraud, Quang Long Nguyen

Efficient Scheme for Chemical Flooding Simulation

Benjamin Braconnier*, Eric Flauraud and Quang Long Nguyen

IFP Energies nouvelles, 1-4 avenue de Bois-Préau, 92852 Rueil-Malmaison Cedex - France
e-mail: benjamin.braconnier@ifpen.fr - eric.flauraud@ifpen.fr - quang-long.nguyen.@ifpen.fr

* Corresponding author

Résumé — **Un schéma numérique performant pour la simulation des écoulements d'agents chimiques dans les réservoirs pétroliers** — Dans cet article, nous proposons un schéma numérique performant pour la simulation des procédés de récupération améliorée utilisant des espèces chimiques. Dans un soucis de clarté, seul le polymère est considéré dans le modèle physique. Ainsi, nous considérons un modèle *black-oil* amélioré par la prise en compte du polymère : une équation de conservation de sa masse et l'effet qu'il occasionne sur la phase eau. Nous supposons que le polymère est transporté dans la phase eau uniquement ou adsorbé sur la roche suivant une isotherme de Langmuir. Pour ce modèle physique, nous proposons un schéma numérique basé sur une technique de pas fractionnaire. La première étape consiste en la résolution du sous système constitué des équations de conservation de la masse des composants lourd, volatile et eau et la deuxième étape est dédiée à la conservation de la masse du polymère. Les matrices issues des formulations implicites conservent une taille réduite préservant ainsi l'efficacité des solveurs linéaires. Cependant, le couplage entre les équations des constituants et du polymère n'est pas complètement résolu. Pour montrer la validité de ce schéma, nous avons développé un schéma explicite pour le polymère. Son critère CFL (Courant-Friedrichs-Levy) contraint de prendre des petits pas de temps ce qui assure une bonne résolution du couplage. Pour valider le schéma implicite, nous avons réalisé quelques simulations utilisant du polymère: le balayage d'une carotte, un 5-spot en présence d'ions et de surfactant et un cas réel tridimensionnel. Des comparaisons sont effectuées entre les schémas explicite et implicite du polymère. Elles montrent que le schéma implicite est efficace, robuste et reproduit bien la physqiue. Les développements et les simulations ont été réalisés avec le logiciel PumaFlow [PumaFlow (2013) Reference manual, release V600, Beicip Franlab].

Abstract — *Efficient Scheme for Chemical Flooding Simulation* — *In this paper, we investigate an efficient implicit scheme for the numerical simulation of chemical enhanced oil recovery technique for oil fields. For the sake of brevity, we only focus on flows with polymer to describe the physical and numerical models. In this framework, we consider a black-oil model upgraded with the polymer modeling. We assume the polymer only transported in the water phase or adsorbed on the rock following a Langmuir isotherm. The polymer reduces the water phase mobility which can change drastically the behavior of water oil interfaces. Then, we propose a fractional step technique to resolve implicitly the system. The first step is devoted to the resolution of the black-oil subsystem and the second to the polymer mass conservation. In such a way, jacobian matrices coming from the implicit formulation have a moderate size and preserve solvers efficiency. Nevertheless, the coupling between the black-oil subsystem and the polymer is not fully resolved. For efficiency and accuracy comparison, we propose an explicit scheme for the polymer for which large time step is prohibited due to its*

CFL (Courant-Friedrichs-Levy) criterion and consequently approximates accurately the coupling. Numerical experiments with polymer are simulated : a core flood, a 5-spot reservoir with surfactant and ions and a 3D real case. Comparisons are performed between the polymer explicit and implicit scheme. They prove that our polymer implicit scheme is efficient, robust and resolves accurately the coupling physics. The development and the simulations have been performed with the software Puma-Flow [PumaFlow (2013) Reference manual, release V600, Beicip Franlab].

INTRODUCTION

Using chemical Enhanced Oil Recovery (EOR) techniques to improve oil recovery in oil fields is a challenging task. With these techniques, from 30% to 60% of the reservoir's initial oil in place can be extracted [1] compared to 10-20% when primary or secondary recovery techniques are used [2]. Chemical EOR techniques consist in chemical injection such as polymers (P), surfactants (S), alkaline (A) or foam (F) depending on the considered case. The chemical effects are usually combined to obtain famous process such as SWAG (Surfactant Water Alterning Gas), FAWAG (Foam Alterning Water Alterning Gas) processes. Thus, one has to determine carefully the necessity of using EOR, and the best operating mode relatively to financial profitability and global problem constraints. For this, reservoir engineers use intensively reservoir simulation software for the experimentation of many exploitation scenarios. Thus, simulation softwares have to be accurate, robust and very efficient. This paper describes the numerical modeling and simulation of chemical injection using the reservoir simulator PumaFlow of *IFP Energies nouvelles* [3]. For the sake of brevity, we focus only on the polymer.

The polymers used in EOR technique are water soluble and have high molecular weight. They are injected in oil field through the wells. They increase the water viscosity and lower the mobility ratio [4, 5]. Thus, water oil interfaces have less instabilities: water fingering and breakthrough are reduced. Thus, the oil recovery is improved as water cut is delayed. Depending on the rock and water phase properties, polymers can be adsorbed on the rock's surface, reducing their benefits on the oil recovery. Ions are also under concern in our model as polymers adsorption depends on salinity.

Usually, these flows are described with a black-oil type system [6] upgraded with the chemicals components mass conservation, adsorption equations and effects on the phases. In fact, in order to preserve the simulator efficiency, compositional models are as far as possible avoided. We suppose that chemical components are only transported in the water phase. The physical model includes specific mathematical difficulties because chemical components effect on the properties of the flow. For the polymer, the mobility reduction depends on various parameters, in particular polymers' non-Newtonian behavior [4, 5]. Thus, devising an accurate, robust and efficient numerical scheme is a challenging task.

In the present paper, we focus on finite volume numerical methods. Initially, because of the complexity of the physical system, numerical methods are based on fractional step techniques. Pressure and eventually saturation are solved implicitly and then chemical components are deduced using explicit numerical schemes [7–9]. This technique leads to severe time step restriction with polymers and numerical simulation at field scale becomes time consuming. In fact, polymers have high molecular mass and size and thus flow faster than other components. Thus, they induce severe CFL (Courant-Friedrichs-Levy) criterion. Fully implicit schemes can been considered. These approaches consider all the dependencies between polymers and other variables. When several chemical species are simulated, the implicit matrices obtained from linearization are composed of full large sized blocks leading to high memory cost and the use of linear iterative solvers becomes less efficient. For this reason, fully implicit schemes have not been investigated yet. In this paper, we experiment an original implicit formulation based on a fractional step technique. The black-oil subsystem and the polymer mass conservation are resolved sequentially. The polymer equation is resolved either explicitly or implicitly. The polymer implicit scheme is stable and preserves linear solver efficiency as jacobian matrices have reduced size. This scheme is robust and allows to take large time steps. However, because of the strong coupling between the black-oil subsystem and the polymer mass conservation, the physics of the coupling is less accurately resolved when large time steps are considered. In this way, we have performed several numerical simulations with polymer: a core flood, a 5-spot reservoir with surfactant and ions and a 3D real case. With these simulations, we prove that the polymer implicit scheme reproduces correctly the physics of the polymer on the flow with a good efficiency.

In Section 1, we present the physical model governing the flow. It is composed of a black-oil subsystem upgraded with the polymer mass conservation equation and the modeling of its effect on the water phase. In Section 2, our numerical schemes are described: an implicit scheme for the black-oil subsystem and either

an explicit or implicit scheme for the polymer mass conservation equation. For the explicit scheme, we exhibit an approximate CFL criterion. Then, in Section 3, we propose several numerical simulations for which we compare the results obtained between the polymer explicit and implicit schemes. We prove our implicit numerical scheme efficient and relevant to reproduce polymer flooding flows.

1 PHYSICAL MODEL

We consider a model for a three-phase flow in a porous medium with polymer. We distinguish three phases: a liquid phase W mainly consisting of water; a second liquid phase O mainly consisting of oil and a gas phase G. This flow is impacted by the presence of a polymer. We suppose the polymer is whether mobile and transported in the water phase only, or fixed and adsorbed on the rock. When present in the water phase, we assume that the polymer mass does not affect the water mass conservation. However, the polymer reduces the water velocity through a mobility reduction factor.

1.1 Modified Black-Oil Model

To describe the water and hydrocarbon phases, we consider a black-oil model [6, 10] where the water phase involves a mobility reduction factor noted R_m which is defined below:

$$
\begin{cases}
\partial_t(\Phi C_h \rho_O S_O) + \nabla \cdot (\rho_O C_h \mathbf{u}_O) + C_h q_O = 0 \\[2mm]
\partial_t(\Phi \rho_G S_G + \Phi C_v \rho_O S_O) + \nabla \cdot (\rho_O C_v \mathbf{u}_O + \rho_G \mathbf{u}_g) \\[1mm]
\qquad\qquad + q_G + C_v q_O = 0 \\[2mm]
\partial_t(\Phi \rho_W S_W) + \nabla \cdot \left(\rho_W \dfrac{\mathbf{u}_W}{R_m} \right) + \dfrac{q_W}{R_m} = 0
\end{cases}
\quad (1)
$$

where Φ is the rock porosity. For each phase denoted $\psi = W, O, G$, S_ψ is the saturation, ρ_ψ is the mass density and q_ψ denotes the source term per volume. It will be useful to discern the outflow source terms $q_\psi^+ \geq 0$ modeling producer wells and the inflow source terms $q_\psi^- \leq 0$ devoted to injector wells. In the following, we suppose that we only inject water in the reservoir: $q_O^- = q_G^- = 0$.

C_h and $C_v = 1 - C_h$ denote respectively the mass fraction of the heavy and volatile components in the oil phase. The volatile component mass transfer between the oil and gas phases is governed by the equilibrium $X_v = 1/K_v$ where K_v is an equilibrium constant depending

on pressure. X_v is the molar fraction of the volatile component in the oil phase defined from C_h and C_v.

Under laminar flow conditions, the pure phase velocities in permeable porous media are governed by generalized Darcy laws:

$$
\begin{cases}
\mathbf{u}_W = -\dfrac{K k r_W}{\mu_W} (\nabla P_W - \rho_W \mathbf{g}) \\[3mm]
\mathbf{u}_O = -\dfrac{K k r_O}{\mu_O} (\nabla P_O - \rho_O \mathbf{g}) \\[3mm]
\mathbf{u}_G = -\dfrac{K k r_G}{\mu_G} (\nabla P_G - \rho_G \mathbf{g})
\end{cases}
$$

where K is the rock permeability, $k r_\psi$ is the relative permeability for the phase ψ, μ_ψ is the pure phase viscosity, P_ψ is the pressure of the phase ψ and $\mathbf{g}$ is the gravity. In order to simplify notations, we introduce the phase mobility $\lambda_\psi = k r_\psi / \mu_\psi$ and the hydrodynamic potential:

$$
\mathbf{v}_\psi = -K(\nabla P_\psi - \rho_\psi \mathbf{g})
$$

such that $\mathbf{u}_\psi = \lambda_\psi \mathbf{v}_\psi$.

1.2 The Polymer Model

The system (1) is completed with the polymer mass conservation equation:

$$
\partial_t(m_p) + \nabla \cdot \left(\rho_W \frac{\mathbf{u}_W}{(1 - \alpha_P) R_m} C^w \right) + \frac{q_W}{R_m} C^w = 0 \quad (2)
$$

where $m_p = \Phi \rho_W S_W C^w + (1 - \Phi) \rho_R C^r$ is the total mass of polymer per unit volume, C^w is the polymer mass fraction in the water, C^r is the polymer mass fraction on the rock and ρ_R is the rock mass density assumed constant. $\alpha_P \leq 1$ is the exclusion volume factor.

Adsorption

We suppose that the polymer adsorption is instantaneous and governed by a Langmuir isotherm [4, 5]. The mass fraction of polymer adsorbed on the rock is defined by:

$$
C^r = q_P^{max} \frac{b C^w}{1 + b C^w} \quad (3)
$$

where b is the Langmuir coefficient and q_P^{max} is the maximal adsorption which may depend on the salinity.

The total mass of polymer m_P is thus related to the mobile polymer mass fraction in the water C^w through the relation:

$$
\begin{aligned}
m_p &= \Phi \rho_W S_W C^w + (1 - \Phi) \rho_R q_P^{max} \frac{b C^w}{1 + b C^w} \\
&= \mathscr{F}(C^w, \Phi, \rho_W, S_W)
\end{aligned}
\quad (4)
$$

where we have introduced the operator $m_p = \mathscr{F}(C^w, \Phi, \rho_W, S_W)$ defined with the previous formula. This operator is invertible with respect to the polymer mass fraction C^w as this variable can be obtained from the total polymer mass by resolving a second order polynomial equation which has a unique positive root. After some calculations, we obtain:

$$C^w = \mathscr{F}^{-1}\left(m_p, \Phi, \rho_W, S_W\right)$$

$$= \frac{\sqrt{\left(\frac{m_W}{b} + m_p - m_R q_P^{max}\right)^2 + 4 m_W q_P^{max}} - \left(\frac{m_W}{b} + m_p - m_R q_P^{max}\right)}{2 m_W}$$

(5)

where $m_W = \Phi \rho_W S_W$ and $m_R = (1 - \Phi)\rho_R$.

Thus, the operator $\mathscr{F}$ defines a bijection between the total mass of polymer m_P and the mobile polymer mass fraction C^w. In order to simplify notations, we omit, from now, the dependence of this operator on the porosity, water density and saturation.

Mobility Reduction Factor

R_m is the mobility reduction induced by the polymer. In fact, the polymer effect can be viewed as an increase of the water viscosity. When water is used to mobilize other phases with high viscosity such as heavy oil, the polymer improves the mobility ratio between water and oil $\lambda_{W,O} = \lambda_W / \lambda_O$ (see [11] for more details). By consequence, the water fingering at the interfaces with oil occurring with unfavorable mobility ratio is reduced or canceled and water breakthrough is delayed. From a production point of view, the water cut is also delayed and oil recovery is thus improved. As polymers can be of different forms such as hydrolyzed polyacrylamide or biopolymer and depend strongly of the regime considered through a non Newtonian behavior, we consider that the mobility reduction is a function of the form:

$$R_m = \frac{R_m^{tab}(C^w, \gamma, I_\mu)}{R_m^{tab}(0, \gamma, I_\mu)} \left(1 + \frac{C^r}{q_P^{max}} \left(\frac{1}{\sqrt{R_m^{tab}(0, \gamma, I_\mu)}} - 1\right)\right)^{-2}$$

R_m^{tab} is a tabulated function deduced from experimental data. It is given from three parameters: the polymer concentration in the water phase C^w, the shear stress γ defined by a analytical correlation:

$$\gamma = \frac{4|\mathbf{u_W}|}{\Phi S_W R_p} \text{ with } R_p = \left(\frac{8|K|kr_W}{\Phi S_W}\right)^{\frac{1}{2}}$$

and the ionic force I_μ which is a function of salinity.

Exclusion Volume

Due to their important size, polymer molecules have a limited access to pore volume [11] and flow usually faster in the water phase. These phenomena depend essentially on the characteristic of the porous media, the polymer type, its concentration and the water phase saturation. These phenomena are usually referred as inaccessible pore volume or exclusion volume. Their modeling is performed by considering a reduction of porosity in the polymer mass balance equation through the parameter α_P. In practice, exclusion volumes are low values and difficult to measure. In our model, we consider a constant exclusion volume factor.

In the next section, we describe the numerical resolution of the system composed of the subsystem (1) and the polymer equation (2). The coupling between the two parts of the system comes from the mobility reduction and the polymer adsorption. This coupling is strong and discussed in the following.

2 DISCRETIZATION AND NUMERICAL SCHEME

2.1 Model Formulation

Before describing our numerical method, let's first discuss about the properties and formulations of the physical model. Composed of hyperbolic and parabolic equations (see [10] for the black-oil system) with additional non linearity due to polymer adsorption and mobility reduction, it is hence hazardous to analyze the model. In fact, the polymer mass conservation and the water phase conservation are fully coupled though the mobility reduction which involves the mobile polymer concentration, adsorption and the flow shear rate. From a physical point of view, the presence of polymer changes drastically the behavior of a flow. It transforms an unstable flow with water fingering and law pressure ratio between producer and injector wells to a stable flow where polymer maintains the water oil interface and increases the pressure ratio between the wells. Thus the underlying physics of the polymer mobility reduction is non linear and of high importance, making the system fully coupled.

In such a context, it is usually recommended to use a fully implicit scheme. In order to have a stable and convergent scheme, all terms must be derived: mobility reduction, shear rate, polymer adsorption isotherm. These terms involve the water saturation, the porosity and the polymer mass fraction yielding to non sparse jacobians. In general, chemical recovery process use several chemical species, for example the A (alkaline) S (surfactant) P (polymer) process. In this case, Jacobian

are non sparse with dimension 6×6 altering the efficiency of the method. Additional derivative calculations become significant, linear systems have high dimension and require more memory and their resolution needs an important amount of additional arithmetic operations.

We suggest to investigate a sequential resolution which enforces the numerical stability and efficiency of the method. In this framework, we propose to resolve the system (1) in two steps: the first step is devoted to the black-oil subsystem and the second step to the polymer mass conservation. In this way, jacobian matrices have a limited size (3×3 or 1×1). The additional derivative calculations are low and the efficiency of the linear solver is preserved. Nevertheless, the coupling of the system is endangered because the coupling between the polymer and the black-oil system is not fully resolved, especially with large time steps. One has to prove by numerical simulation that this method resolves accurately the physics of the flows.

For the polymer mass conservation equation, several unknowns can be chosen for the resolution. In fact, this equation can be formulated with the total polymer mass in each bulk volume:

$$\partial_t(m_P) + \nabla \cdot \left(\frac{\rho_W \mathbf{u}_W \mathscr{F}^{-1}(m_p)}{(1 - \alpha_P) R_m(\mathscr{F}^{-1}(m_p))} \right)$$
$$+ \frac{q_W^+ \mathscr{F}^{-1}(m_p)}{R_m(\mathscr{F}^{-1}(m_p))} + \frac{q_W^-(C^w)^{inj}}{R_m((C^w)^{inj})} = 0$$

where $(C^w)^{inj}$ denotes the polymer mass fraction in the injected water. For this formulation, non linearities related to adsorption and mobility reduction are contained in the space derivatives. Thus, time discretization is still simple leading to a scheme with low mass balance error.

The polymer total mass conservation can also be rewritten with the mobile polymer mass fraction in water, yielding the equation:

$$\partial_t(\mathscr{F}(C^w)) + \nabla \cdot \left(\frac{\rho_W \mathbf{u}_W C^w}{(1 - \alpha_P) R_m(C^w)} \right)$$
$$+ \frac{q_W^+ C^w}{R_m(C^w)} + \frac{q_W^-(C^w)^{inj}}{R_m((C^w)^{inj})} \qquad = 0$$

Despite this formulation looks more simple, the time dicretization involves some non linear terms, making the scheme less reliable in term of mass conservation. In the case where the non linearity becomes significant, the scheme might generate polymer mass conservation loss. This formulation will not be used.

In the following subsections, we detail the resolution of the black-oil subsystem and of the polymer mass

conservation. The black-oil subsystem resolution is based on an implicit scheme and the polymer is resolved explicitly or implicitly.

2.2 Domain Discretization

Let $\mathscr{M}_h$ be an admissible finite volume mesh of the reservoir given by a family of control volumes or cells noted K. For any K of $\mathscr{M}_h$, $|K|$ is its measure, $KL = \partial K \cap \partial L$ is the common interface between K and L and $\mathbf{n}_{KL}$ denotes the unit normal vector to the interface KL outward to K. The set of neighbors of the cell K is denoted by $\mathscr{N}(K)$, that is $\mathscr{N}(K) = \{L \in \mathscr{M}_h; \partial K \cap \partial L \neq \emptyset\}$.

Π_{prod} is the set of perforations of the producer wells and Π_{inj} is the set of of perforations of the injector wells and M is the set of all the corresponding perforated cells in $\mathscr{M}_h$. For instance, K is a perforated cell if it exists a perforation $j \in \Pi_{prod}$ or $j \in \Pi_{inj}$ such that $M(j) = K$.

Finally, we introduce an increasing sequence of discrete times $\{t^n\}_{0 \leq n \leq N}$ such that $t^0 = 0$ and $t^N = T$. Then, the time interval $(0, T)$ is subdivided into N variable time steps $\Delta t = t^{n+1} - t^n$, $0 \leq n \leq N - 1$.

2.3 Water and Hydrocarbons Mass Conservation

For the water and hydrocarbon components mass conservation equations discretization, we use an implicit scheme in time and an upwind finite volume method for the spatial derivatives:

See Equation (6)

where $\mathbf{v}_{\psi,KL}^{n+1}$ is a finite volume discretization of the flux $\int_{KL} \mathbf{v}_\psi \cdot \mathbf{n}_{KL} d\sigma$ at the time $t = t^{n+1}$. For each phase, we define the operator:

$$(\mathbf{v}_{\psi,KL})^+ = \max(0, \mathbf{v}_{\psi,KL}) \text{ and } (\mathbf{v}_{\psi,KL})^- = \min(0, \mathbf{v}_{\psi,KL})$$

in order to have the upwind scheme. Except the reduction mobility factor, the numerical scheme is classical and addressed in the literature [10].

In a fully implicit scheme, the mobility reduction factor should be set as:

$$(R_m)_K^l = (R_m)_K^{n+1}$$
$$= R_m\left(\mathscr{F}^{-1}((m_p)_K^{n+1}), (\Phi)_K^{n+1}, (\rho_W)_K^{n+1}, (S_W)_K^{n+1}\right)$$

yielding a fully complete 4×4 Jacobian in our context. As it is mentioned in the previous section, this scheme efficiency can be reduced depending of the context because of the memory needed, derivatives calculation and Newton convergence. Thus, we propose to discretize

$$
\begin{cases}
|K|\dfrac{(\Phi\rho_O S_O)_K^{n+1}-(\Phi\rho_O S_O)_K^{n}}{\Delta t}+\displaystyle\sum_{L\in\mathcal{N}(K)}(\rho_O\lambda_O C_h)_K^{n+1}(\mathbf{v}_{O,KL}^{n+1})^{+}+(\rho_O\lambda_O C_h)_L^{n+1}(\mathbf{v}_{O,KL}^{n+1})^{-}\\[2mm]
\qquad+\displaystyle\sum_{j\in\Pi_{prod}|M(j)=K}(C_h)_K^{n+1}Q_{O,j}^{+,n+1}=0\\[4mm]
|K|\dfrac{(\Phi\rho_O C_v S_O\ +\ \Phi\rho_G S_G)_K^{n+1}-(\Phi\rho_O C_v S_O\ +\ \Phi\rho_G S_G)_K^{n}}{\Delta t}+\displaystyle\sum_{L\in\mathcal{N}(K)}(\rho_O\lambda_O C_v)_K^{n+1}(\mathbf{v}_{O,KL}^{n+1})^{+}+(\rho_O\lambda_O C_v)_L^{n+1}(\mathbf{v}_{O,KL}^{n+1})^{-}\\[2mm]
\qquad+\displaystyle\sum_{L\in\mathcal{N}(K)}(\rho_G\lambda_G)_K^{n+1}(\mathbf{v}_{G,KL}^{n+1})^{+}+(\rho_G\lambda_G C_v)_L^{n+1}(\mathbf{v}_{G,KL}^{n+1})^{-}+\displaystyle\sum_{j\in\Pi_{prod}|M(j)=K}\left(Q_{G,j}^{+,n+1}+(C_v)_K^{n+1}Q_{O,j}^{+,n+1}\right)=0\\[4mm]
|K|\dfrac{(\Phi\rho_W S_W)_K^{n+1}-(\Phi\rho_W S_W)_K^{n}}{\Delta t}+\displaystyle\sum_{L\in\mathcal{N}(K)}\dfrac{(\rho_W\lambda_W)_K^{n+1}}{(R_m)_K^{l}}(\mathbf{v}_{W,KL}^{n+1})^{+}+\dfrac{(\rho_W\lambda_W)_L^{n+1}}{(R_m)_L^{l}}(\mathbf{v}_{W,KL}^{n+1})^{-}+\displaystyle\sum_{j\in\Pi_{prod}|M(j)=K}\dfrac{Q_{W,j}^{+,n+1}}{(R_m)_j^{l}}\\[4mm]
\qquad+\displaystyle\sum_{j\in\Pi_{inj}|M(j)=K}\dfrac{Q_{W,j}^{-,n+1}}{(R_m)_j^{l}}=0
\end{cases}
\tag{6}
$$

explicitly the mobility reduction factor so that the polymer mass equation can be resolved separately:

$$
(R_m)_K^{l}=(R_m)_K^{n}\\
=R_m\big(\mathscr{F}^{-1}((m_p)_K^{n}),(\Phi)_K^{n},(\rho_W)_K^{n},(S_W)_K^{n}\big)
$$

As the mobility reduction factor is explicitly resolved, the resolution of the system (6) is classical. For the resolution of the polymer mass fraction, we detail in the next sections two types of decoupled resolution, an explicit scheme or an implicit scheme.

2.4 Polymer Explicit Scheme

Once the black-oil subsystem (6) has been resolved and the updated composition, saturation, density, pressure and porosity have been obtained, one has to consider the polymer mass conservation equation. The first scheme proposed is explicit and resolved with the variable m_P: the total mass of polymer in each grid cell. The explicit scheme writes as follows:

$$
|K|\dfrac{(m_P)_K^{n+1}-(m_P)_K^{n}}{\Delta t}\\[2mm]
+\displaystyle\sum_{L\in\mathcal{N}(K)}\left(\dfrac{\mathscr{F}^{-1}(m_p)}{(1-\alpha_P)R_m}\right)_K^{n}(\rho_W\lambda_W)_K^{n+1}(\mathbf{v}_{W,KL}^{n+1})^{+}\\[2mm]
+\left(\dfrac{\mathscr{F}^{-1}(m_p)}{(1-\alpha_P)R_m}\right)_L^{n}(\rho_W\lambda_W)_L^{n+1}(\mathbf{v}_{W,KL}^{n+1})^{-}\\[4mm]
+\displaystyle\sum_{j\in\Pi_{prod}|M(j)=K}Q_{W,j}^{-,n+1}\left(\dfrac{\mathscr{F}^{-1}(m_p)}{R_m}\right)_K^{n}+\displaystyle\sum_{j\in\Pi_{inj}|M(j)=K}Q_{W,j}^{+,n+1}\left(\dfrac{C^w}{R_m}\right)_j^{inj}
\tag{7}
$$

where we took:

$$
\begin{cases}
\left(\mathscr{F}^{-1}(m_p)\right)_K^{n}=\mathscr{F}^{-1}\left((m_p)_K^{n},(\Phi)_K^{n},(\rho_W)_K^{n},(S_W)_K^{n}\right)\\[2mm]
(R_m)_K^{n}=R_m\left(\left(\mathscr{F}^{-1}(m_p)\right)_K^{n},(\Phi)_K^{n},(\rho_W)_K^{n},(S_W)_K^{n}\right)
\end{cases}
$$

Let remark that the mobility reduction has to be taken entirely at time $t=t^n$ in order to be consistent with the black-oil subsystem resolution.

Once the total mass $(m_p)_K^{n+1}$ has been computed, we deduce the new values of the mobile mass fraction $(C^w)_K^{n+1}$ from Equation (5) and the adsorbed mass fraction $(C^r)_K^{n+1}$ from Equation (3).

This explicit scheme (7) is obviously submitted to a CFL criterion. However, as the polymer velocity is not a divergence free field, it is not possible to derive a L^{∞} stability criterion such as the method described in [12]. Instead, we propose a Von Neumann stability analysis which provides the stability criterion for the polymer scheme:

$$
\Delta t\le\min_{K\in\mathcal{M}_h}\left(\dfrac{|K|A_K^{n}}{\displaystyle\sum_{L\in\mathcal{N}(K)}\dfrac{(\rho_W\lambda_W)_K^{n+1}(\mathbf{v}_{W,KL}^{n+1})^{+}}{1-\alpha_P}+\displaystyle\sum_{j\in\Pi_{prod}|M(j)=K}Q_{w,j}^{+,n+1}}\right)
\tag{8}
$$

with

$$
A=\dfrac{1}{1-\dfrac{1}{R_m}\left(\dfrac{\partial R_m}{\partial C^w}\right)}\ \dfrac{2m_W}{1+\dfrac{\frac{m_W}{b}+m_p-m_R q_P^{max}}{\sqrt{\left(\frac{m_W}{b}+m_p-m_R q_P^{max}\right)^2+4m_W q_P^{max}}}}
$$

where all the values involved in this relation have to be taken at time $t=t^n$ and cell K to obtain A_K^{n}. The first fraction is imputed to the mobility reduction: it can relax or constraints the maximum time step depending on the

mobility reduction curve and regime considered. The second fraction is related with adsorption and relaxes the CFL criterion as the more the polymer is adsorbed the more stable is the scheme.

This CFL criterion makes the entire scheme relevant because large time steps are prohibited. The approximation made on the mobility reduction does not impact significantly the results. Non linearity is sufficiently sampled and physical effects are correctly reproduced as shown in Section 3.

2.5 Polymer Implicit Scheme

We now propose to develop a more efficient scheme for the polymer mass conservation. We suggest to avoid the nonlinearities related to the adsorption and to the mobility reduction factor. In this way, the numerical scheme devoted to the polymer mass conservation is decomposed relatively to a fractional step method. In a first step, we resolve implicitly the polymer flow in the water whereas the adsorption is frozen. The polymer mobile equation can be rewritten and resolved with the mobile polymer mass fraction in water as unknown:

$$
\begin{aligned}
&|K| \frac{(m_W)_K^{n+1}(C^w)_K^{n+1/2} - (m_W C^w)_K^n}{\Delta t} \\
&+ \sum_{L \in \mathcal{N}(K)} \frac{(C^w)_K^{n+1/2}}{(1-\alpha_P)(R_m)_K^n}(\rho_W \lambda_W)_K^{n+1}(\mathbf{v}_{W,KL}^{n+1})^+ \\
&+ \frac{(C^w)_L^{n+1/2}}{(1-\alpha_P)(R_m)_L^n}(\rho_W \lambda_W)_L^{n+1}(\mathbf{v}_{W,KL}^{n+1})^- \\
&+ \sum_{j \in \Pi_{prod}|M(j)=K} Q_{W,j}^{+,n+1} \frac{(C^w)_K^{n+1/2}}{(R_m)_K^n} \\
&+ \sum_{j \in \Pi_{inj}|M(j)=K} Q_{W,j}^{-,n+1}\left(\frac{C^w}{R_m}\right)_j^{inj} = 0
\end{aligned}
$$

where the subscript $n+1/2$ denotes the solution of this first step.

This scheme is linear in the variable $(C^w)_K^{n+1/2}$ which enables robustness, stability and efficiency. The use of the Newton's algorithm is not necessary. In addition, it makes the scheme preserve exactly the global mass balance.

Let note that preserving the consistency with the scheme (6) imposes to resolve explicitly the mobility reduction in the polymer mass conservation.

The second step yields the final solution and is devoted to the resolution of the Langmuir isotherm by computing the new equilibrium:

$$(C^w)_K^{n+1} = \mathscr{F}^{-1}\left((m_W)_K^{n+1}(C^w)_K^{n+1/2} + (m_R)_K^n(C^r)_K^n\right)$$

from which we deduce the updated total polymer mass with Equation (4). Finally, the adsorbed mass fraction $(C^r)_K^{n+1}$ is computed in each grid block using Equation (3).

In the first step of the scheme, the mobility reduction is taken explicit and it conducts to a CFL criterion. It is possible to formally derive a Von Neumann approach stability analysis but because of its implicit/explicit structure, the CFL criterion is obtain after matrices inversion and diagonalizing. Computing such criterion has not been considered in practice because it is time consuming. By construction, the second step is a projection operator and is not submitted to a CFL criterion. However, the approximation performed: explicit mobility reduction and fractional step technique can deteriorate the resolution of physics and bring numerical diffusion. In Section 3, we prove that our scheme is very efficient and that the physics is accurately resolved.

3 NUMERICAL VALIDATION

3.1 Polymer Core Flood

To validate our implicit method, we consider a one-dimensional numerical test which highlights the properties of the implicit numerical scheme. For this, we choose the injection of a polymer slug followed by chase-water in a carrot. To put into perspective the benefit of polymer on the oil flow rate and cumulative oil production, we also performed the experiment with a tracer instead of the polymer. A tracer is a passive chemical component which does not affect the flow. A very simple type tracer is a dye. From a mathematical point of view, tracers are governed by Equation (2) without adsorption, mobility reduction and exclusion volume (set $R_m = 1$, $\alpha_P = 0$ and $q_P^{max} = 0$). They are numerically resolved with the same technique as polymers. We consider the results of polymer or tracer explicit resolution as reference to validate our implicit scheme.

The domain is a parrallelepipedic pore volume with dimensions $L_x = 100\,\text{m}$, $L_y = L_z = 1\,\text{m}$, a first well in $x = 0\,\text{m}$ for injection and a second well in $x = 100\,\text{m}$ for production. In this medium, the porosity is constant $\Phi = 0.20$ D. At initial time, the volume is uniformly saturated with oil $S_o = 0.85$. At time $T_0 = 0\,\text{d(day)}$, we inject water containing a polymer or a tracer at mass concentration $C^w = 500\,\text{ppm}$ through the first well. Water viscosity is only modified by the polymer which can be linearly increased by a factor 4 with the shear stress and by a factor 10 at the polymer concentration $C^w = 500\,\text{ppm}$. The injection is performed until $T_1 = 81.25\,\text{d}$ with the flow rate $Q = 0.032\,\text{m}^3.\text{d}^{-1}$.

Then, the injection is continued at the same flow rate but with pure water until the final time $T_f = 3\,125\,\mathrm{d}$. For the second well, the flow rate is imposed at a given value Q. The adsorption phenomenon is neglected for this test case.

Considering the flow rate constant in time and through the carrot and fluid incompressible, this case can be described with dimensionless data [13, 14] . For this, we introduce the time $\tau = \Phi L_x L_y L_z / Q = 625\,\mathrm{d}$ corresponding to the time needed for the injection of one pore volume in the reservoir at the flow rate Q.

This experiment is reproduced considering a one dimensional reservoir model with $N_x = 1\,000$, $N_y = N_z = 1$. The simulation is performed using a fully implicit solver [8] except for the polymer or tracer. These components are either resolved explicitly with CFL criterion about 1 or implicitly with CFL criterion about 1 or 10. The computations are done on a standard PC with one processor of an Intel Xeon(R) CPU 2.67 GHz. In Table 1, we summarize all the cases and give some numerical data.

Note that for CFL = 1, implicit and explicit schemes run with very similar computational time. In fact, the implicit scheme requires the calculation of the implicit matrix, its storage and the linear system resolution. Indeed, the extra cost of solving the linear system is low because for small time step, convergence is obtained after only one iteration of the IFPEN solver [15].

In Figure 1, we plot the dimensionless oil flow rate and cumulative oil production for each run. The implicit

TABLE 1

Time simulation results for 1D test case

Component	Resolution	CFL	T CPU (s)	Nstep
Polymer	Explicit	≈ 1	246	12 548
Polymer	Implicit	≈ 1	241	12 548
Polymer	Implicit	≈ 10	33.5	1 367
Tracer	Explicit	≈ 1	240	12 548
Tracer	Implicit	≈ 1	34.4	1 367

resolution of polymer leads to results with more numerical diffusion as it can be seen in the spreading of the front located at time $t = 0.4\tau$. For the case implicit with CFL ≈ 10, the oil production is slightly overestimated on the time interval $(0.2\tau, 0.4\tau)$ but this has no significant effect on cumulative oil production. For the cases with tracer, as the tracer has no effect on the flow, the additional numerical diffusion is produced by the implicit resolution of pressure and saturation. Despite, this numerical diffusion is not so visible because the curves do not have discontinuities. Then we show in Figure 2, the dimensionless component flow rate at the producer well and the component cumulative mass production. These curves put into perspectives the additional numerical diffusion of the implicit scheme. Despite, the solution is still accurate: front location and mass balance.

This test validates the implicit resolution of polymer. This scheme is robust and allows to pass through
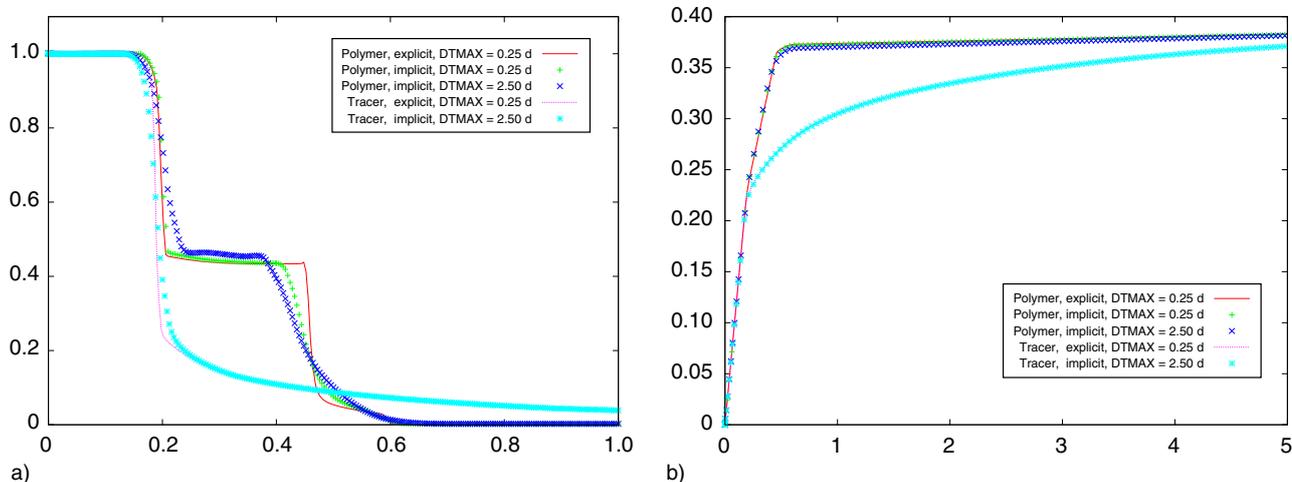

Figure 1

a) Dimensionless (by the total flow rate Q) oil flow rate at the producer well at *in situ* condition *versus* dimensionless time.

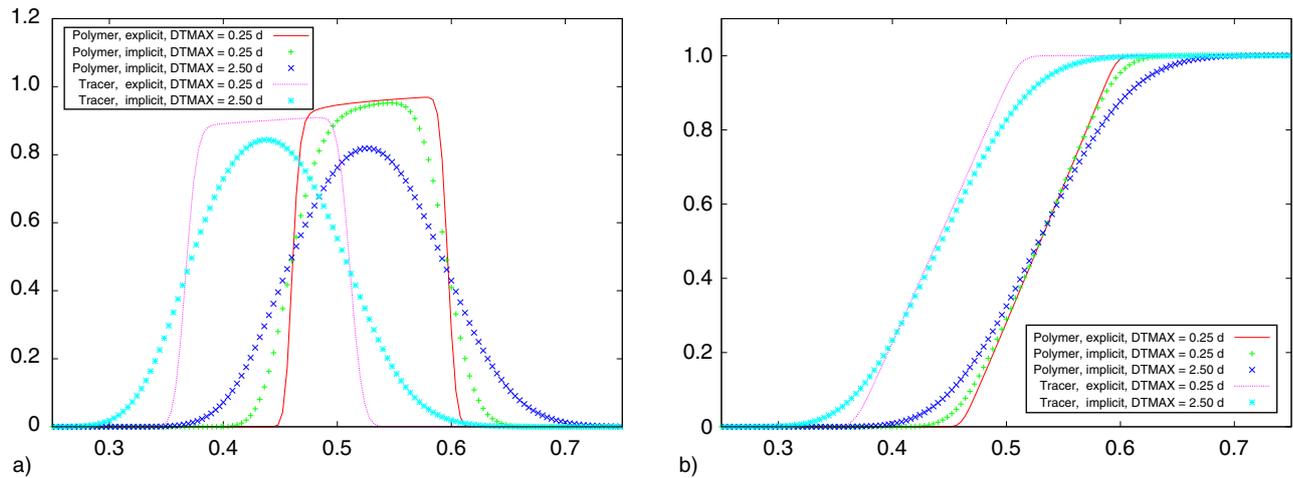b) Dimensionless (by the initial oil in place) cumulative oil produced *versus* dimensionless time.

Figure 2

a) Dimensionless (by the polymer concentration injected) polymer concentration at the producer well *versus* dimensionless time.

b) Dimensionless (by the total polymer mass injected) cumulative polymer mass at the producer well *versus* dimensionless time.
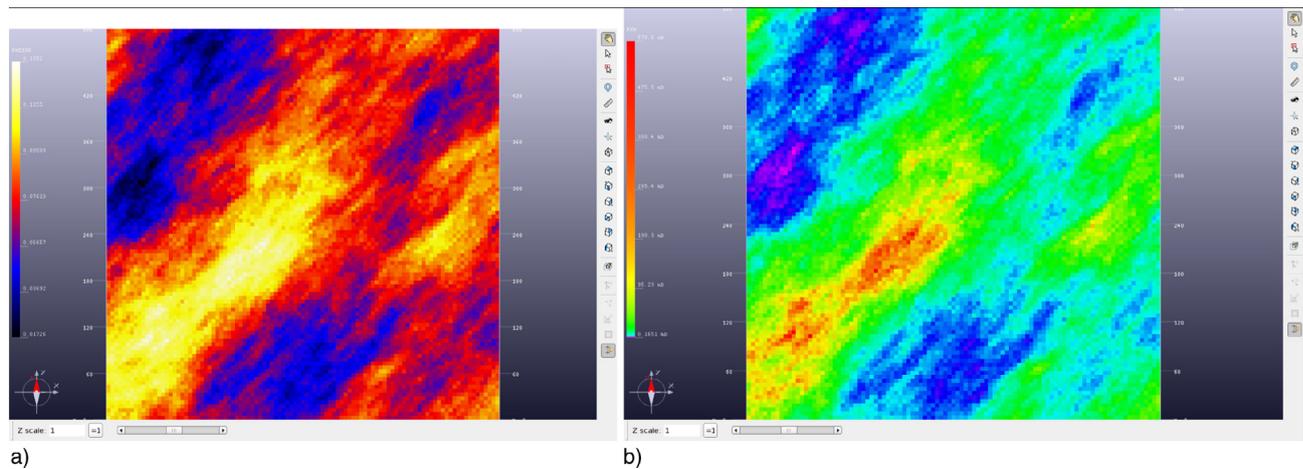

Figure 3

a) Initial distribution of porosity and b) permeability in *x* direction of the 5-spot 2D reservoir.

10 times the explicit CFL criterion (8). The numerical diffusion is not negligible but does not modify the accuracy of the results: front location, mass conservation, cumulative production.

3.2 Polymer Surfactant and Ions in a 5-Spot Reservoir

We study now another test case with SP (Surfactant-Polymer) flood. It consists of a 5-spot reservoir with only one layer vertically. The mesh reservoir is composed of one bloc in *z* direction and 101 blocs in both *x* and *y*

directions. The dimensions are: $L_x = L_y = 5\,\mathrm{m}$ and $L_z = 10\,\mathrm{m}$. The medium is heterogeneous with porosity varying from 0.017 to 0.14 and permeability varying from 0 and 570 mD (*Fig. 3*). The initial irreducible water saturation is equal to 0.23 and the initial residual oil saturation is equal to 0.32. The temperature of the reservoir is about 85°C with 214 bar for average pressure. There are four wells injector in each corner of the reservoir and only one well injector in the center.

Surfactant data (permeability-capillary pressure curves modification, adsorption) as well as polymer data

TABLE 2

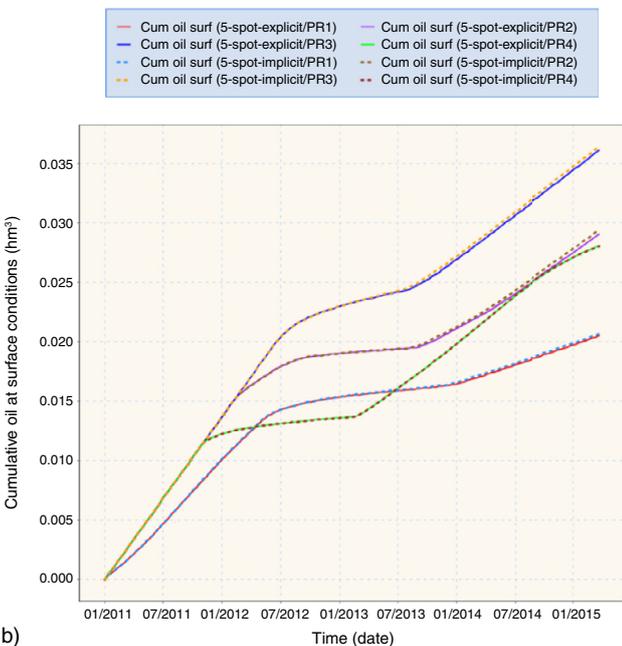5-spot SP flood injection schedule

Time (days)	Surfactant slug (ppm)	Polymer slug (ppm)	Salinity (g/L)
Until 513	0	0	1
Until 899	8 000	2 000	1
Until 1 541	0	2 000	1

TABLE 3

Time simulation results for 2D 5-spot test case

Component	Polymer	Polymer
Resolution	Explicit	Implicit
ΔT max	2 days	2 days
T CPU	1 h 11 min 25 s	26 min 40 s
Nstep	48 715	3 624
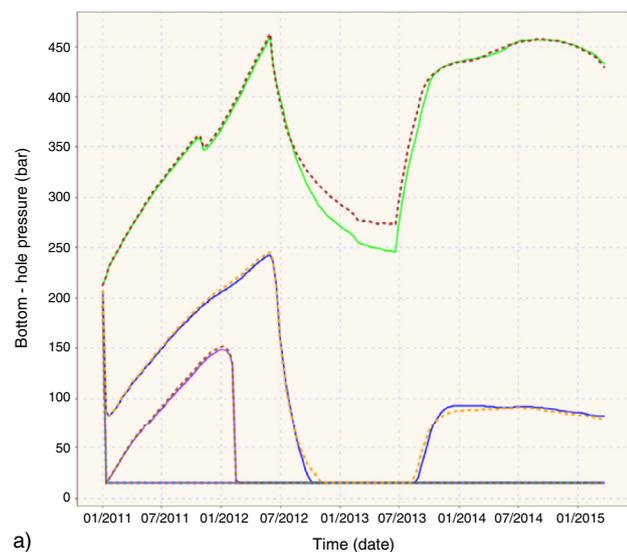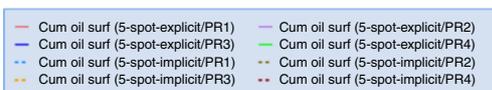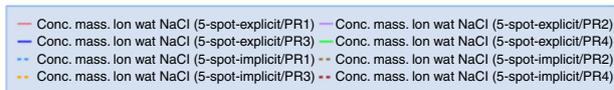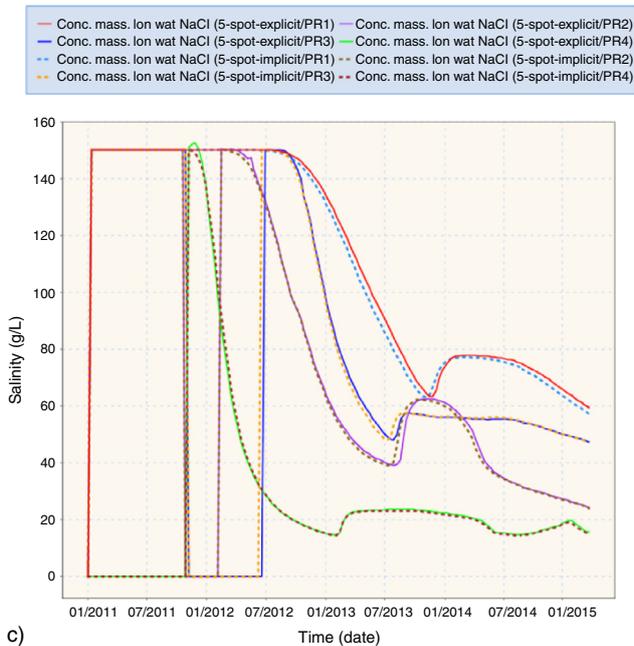
Figure 4

Production results of the 2D 5-spot test case. a) bottom-hole pressure, b) cumulative oil at surface condition, c) salinity.
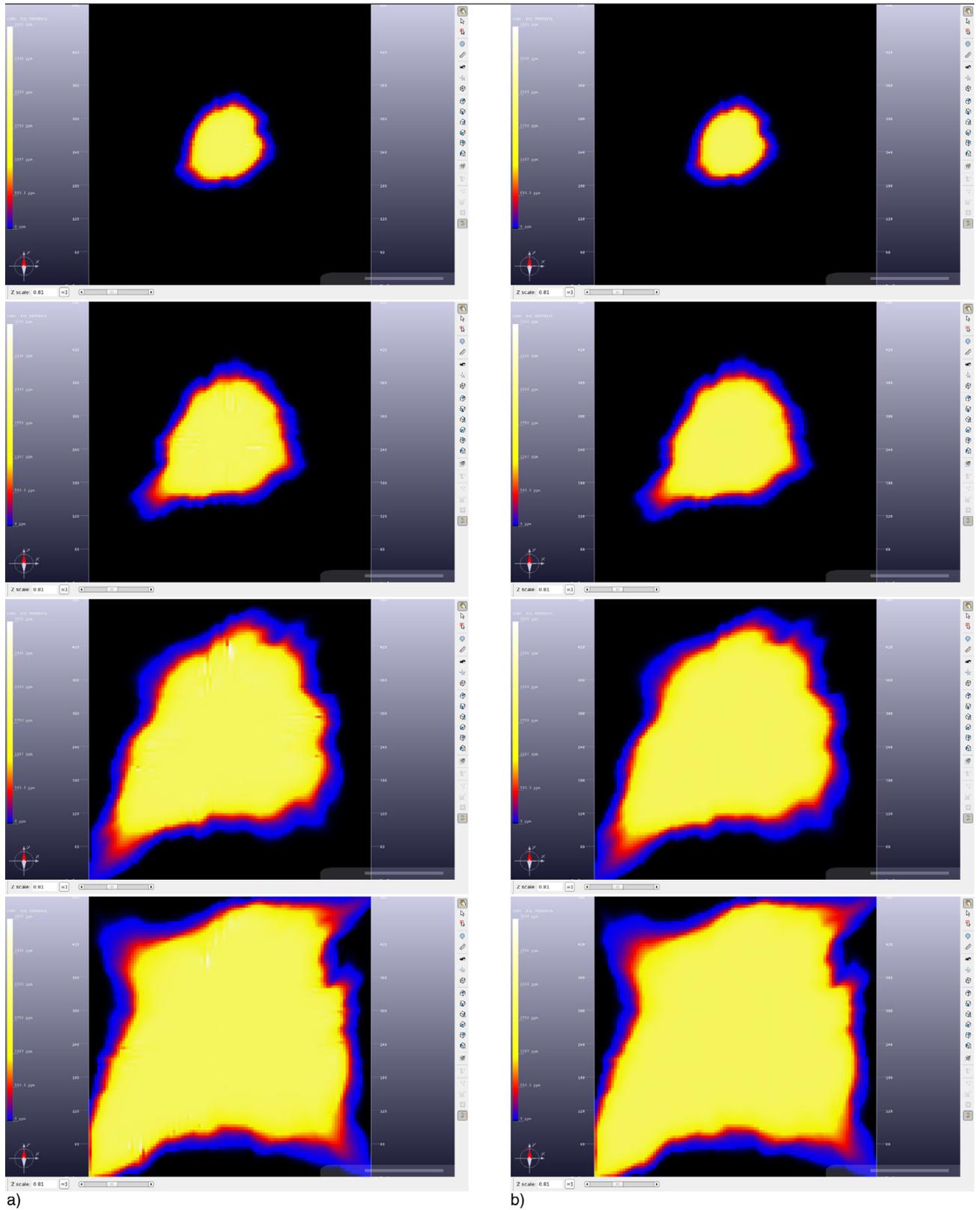
Figure 5

Grid production results for a) explicit and b) implicit schemes – mass concentration of polymer at different time – 5-spot case.
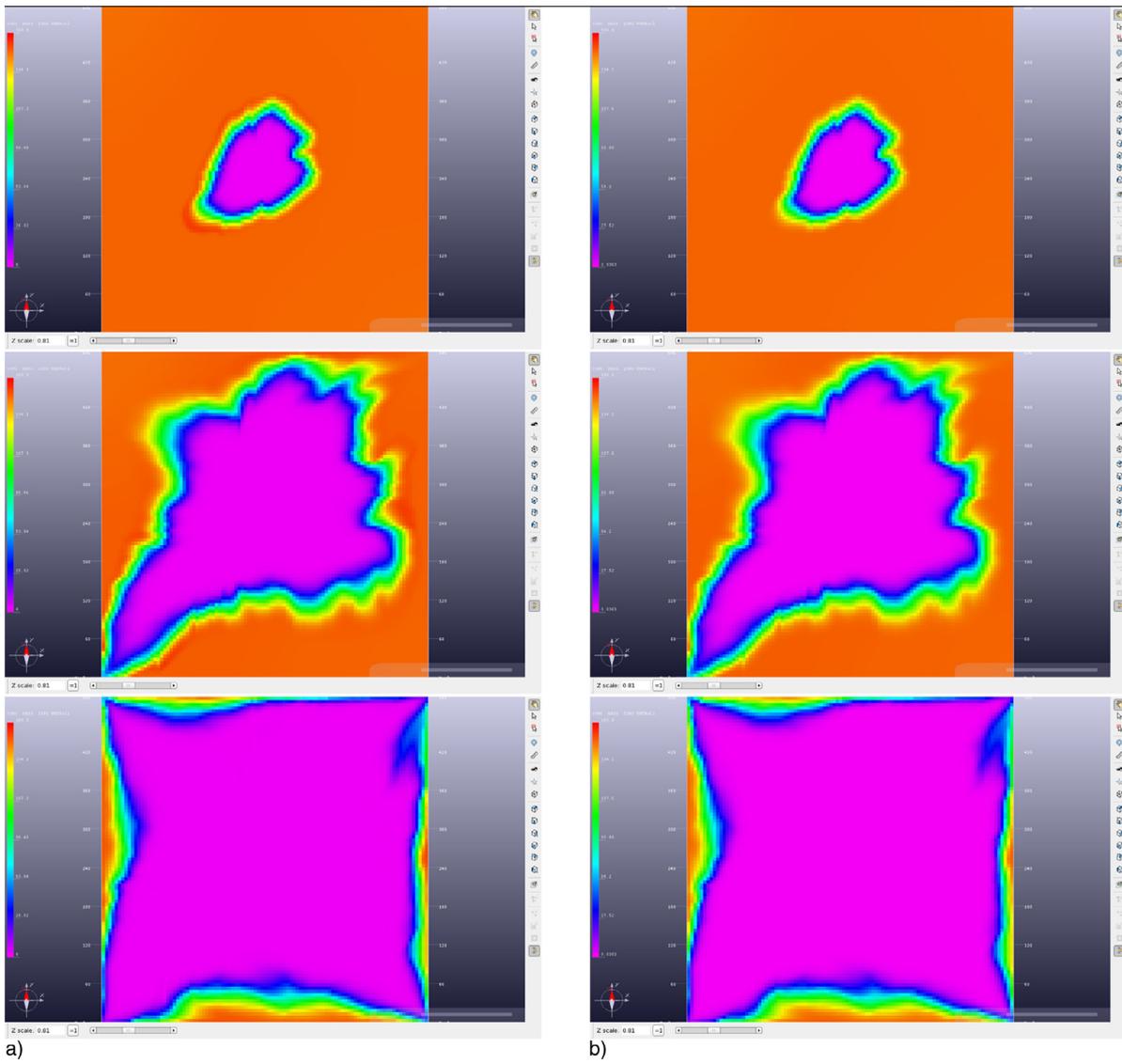
Figure 6

Grid production results for a) explicit and b) implicit schemes – salinity at different time – 5-spot case.
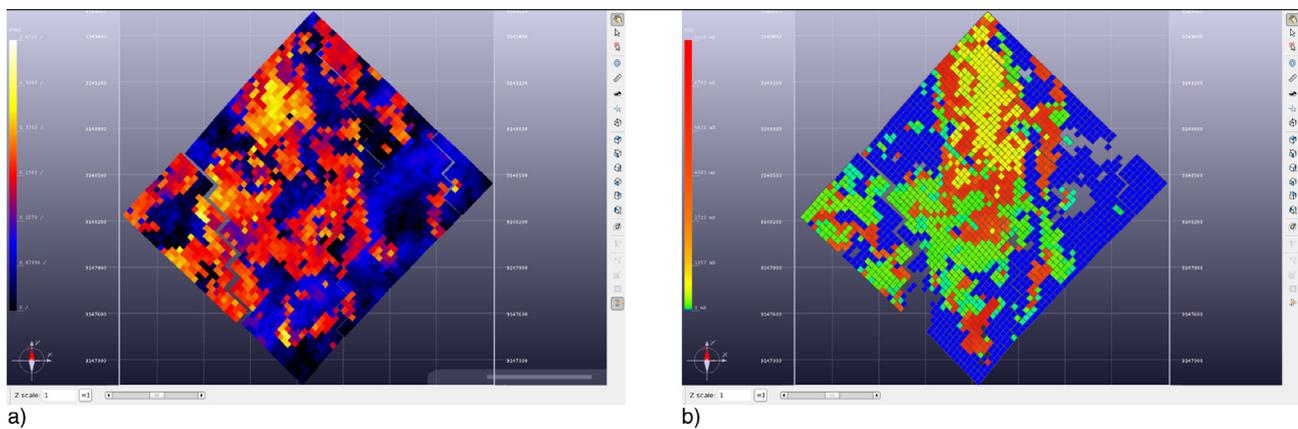

Figure 7

Initial distribution of porosity a) and permeability in *x* direction b).

mobility reduction table are considered. At the initial state, brine is present in the reservoir with a salinity around 150 g/L. In the simulations of this test case we inject a SP flood with brine, the schedule is summarized in Table 2. Note that chemical species and brine are treated in the same way for each scheme, *i.e.* explicit and implicit.

TABLE 4

Time simulation results for 3D test case

Component	Polymer	Polymer
Resolution	Explicit	Implicit
CFL	1 day	10 days
T CPU (s)	26 677	3 402
Nstep	12 423	1 384

We summarize the time simulation results in Table 3. We obtain a gain about 2.7 with implicit scheme compare to the explicit one. Indeed, implicit treatment permits to have larger time steps while still satisfying all constraints (pressure and saturation maximal variation for example). Consequently, the number of time steps is 13 times less with the implicit scheme and the simulation is much faster.

Figure 4 reports some numerical results for producer wells: bottom-hole pressure, cumulative oil at surface condition and salinity. We can see that all variables have good agreement between the two schemes.

Figures 5 and 6 show the propagation of the polymer and salinity in the reservoir along time. Here again, we have good precision of the transport of polymer and salt between implicit and explicit schemes.
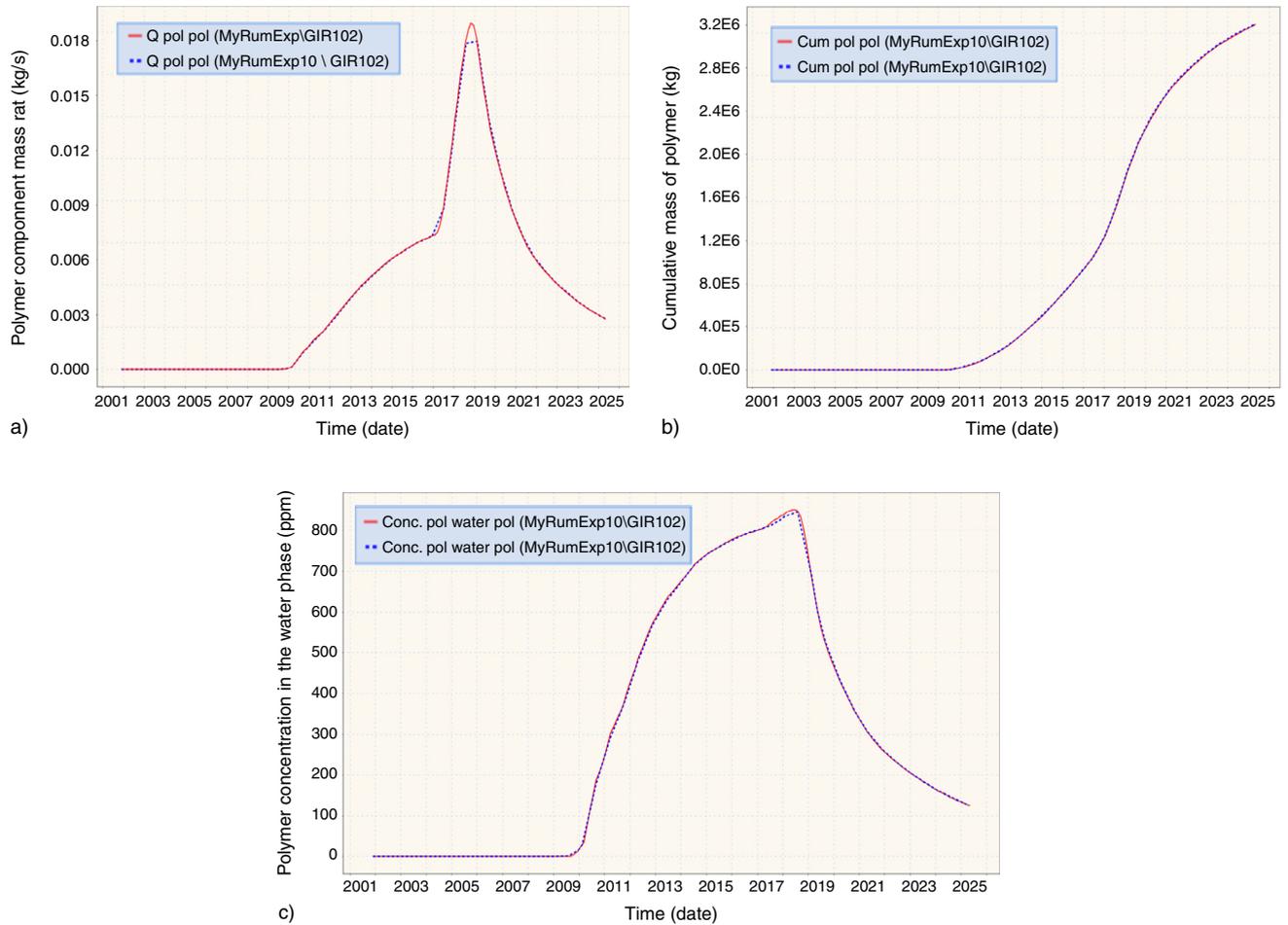

Figure 8

Well production results of explicit (red) and implicit (blue) schemes: a) mass flow rate, b) cumulative mass and c) mass concentration of the polymer component.
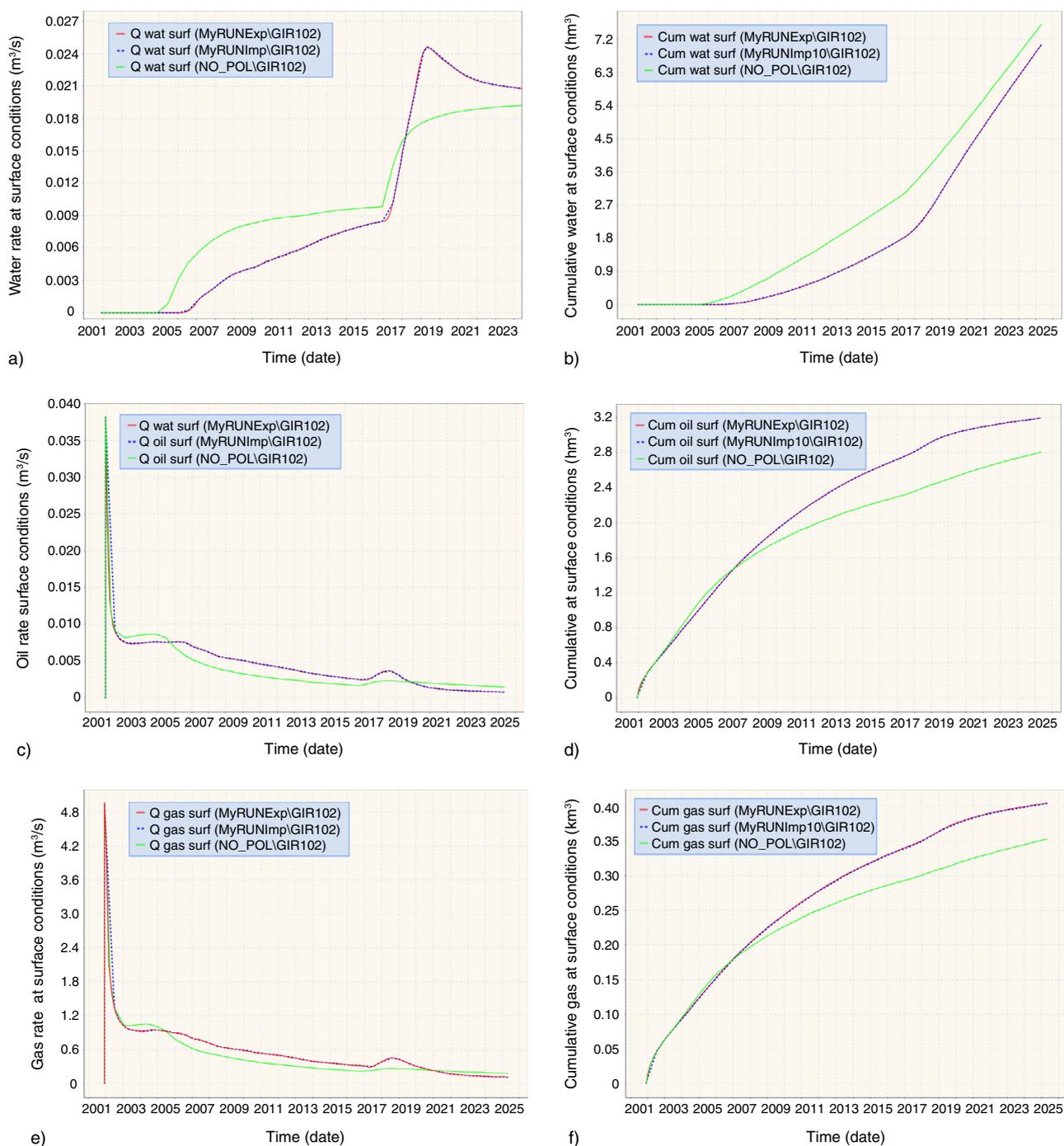
Figure 9

Well production results of explicit (red) and implicit (blue) schemes, comparison between polymer and tracer injections: surface volume rate and cumulative mass production of water, oil and gas components.

3.3 3D Real Case

To enhance our implicit scheme for polymer treatment, we will now present some numerical results of a three-dimensional real test case. We consider a reservoir modeled by a mesh defined in corner point geometry by $47 \times 50 \times 45$ blocs in the directions (x, y, z). The dimension of each bloc is $L_x = L_y = 25$ m and $L_z = 1.2$ m approximately. The reservoir contains some faults and the medium is heterogeneous (porosity values
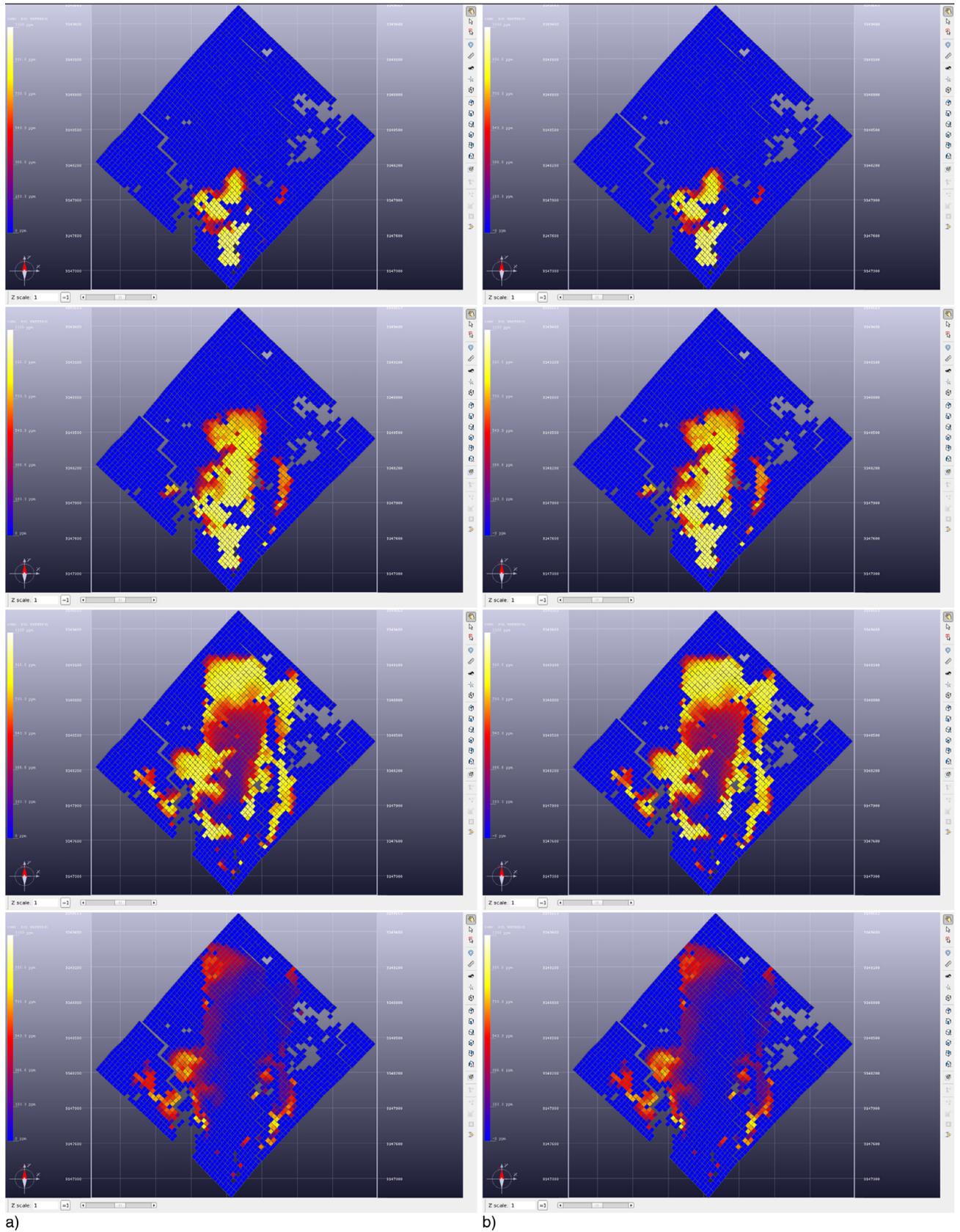
a)

b)

Figure 10

Grid production results for a) explicit and b) implicit schemes – mass concentration of polymer at different time.

between 3.6×10^{-7} and 0.47 and permeability values in x-axis between 0 and 8 140 mD, *Fig. 7*) with three-phase flows, *e.g.* water-oil-gas. The irreducible water saturation is equal to 0.10162 and the residual oil saturation is equal to 0.20113. Capillary pressure is taken into account in the model. There are one well injector and one well producer, both of them are of opposite sides in the reservoir. These wells obey different flow rate and pressure constraints. Note that pressure constraint is relaxed for well injector to maintain same flow rates and consequently same volumes of injected fluid for comparison reason. For this test case, adsorption phenomenon is activated with $q_P^{max} = 20 \mu g/g$ of rock and exclusion volume factor is taken equal to 0.05.

After 11 days of natural depletion production, we inject a slug of water containing polymer during 15 years followed by a slug of chase-water (without polymer) during 9 years. The mass concentration of the polymer in the injected water is $C^w = 1\,000$ ppm which leads to a reduction viscosity by a factor 6 with regard to the given mobility reduction table. Adsorption is neglected in the simulations.

We first do a simulation with the explicit scheme of polymer, then we make use of the implicit scheme on this component to improve the simulation performance. For the explicit resolution, the CFL criterion is equal to 1 to assure the stability, while for the implicit resolution it is equal to 10. A simulation with a tracer instead of the polymer is also presented for comparison with polymer injection. The computations are done in the same configuration has the previous test cases. Time numerical results are shown in Table 4.

Despite time consumed for calculation of the implicit matrix and its linear resolution, the implicit scheme is 7.8 times faster than the explicit one.

Other numerical results for this test case are presented in Figures 8 and 9 (well production results) and 10 (grid flow results). We can see good agreement between explicit and implicit schemes. On the contrary of the first 1D test case, numerical diffusion is not significant for this 3D test case as all fronts superpose. Note that in Figure 9 we also show green curves, results of tracer injection simulation. As tracer has no effect on flow properties, these curves correspond to a simple chase-water simulation, *i.e* without chemical injection. We can see that we obtain a better oil and gas production with polymer/surfactant injection which demonstrates a great interest of EOR injection for enhanced oil recovery.

CONCLUSION AND PERSPECTIVES

In the context of chemical EOR, we have proposed an implicit scheme for the resolution of chemical species.

The implicit scheme is based on a fractional step technique. A first step is devoted to the resolution of the component mass conservation and the second step to the polymer mass conservation. This technique makes the scheme efficient and robust with large time steps. However the coupling between the phases and the polymer mass conservation is not fully resolved. We have proved by numerical simulations that our scheme resolves accurately this coupling with large time steps. For the core flood case, numerical diffusion is more important but the solution still than an accurate behavior: front location and good mass conservation. For the reservoir scale cases, the results obtained with the polymer explicit and implicit schemes are in very good agreement, especially the polymer concentration in the reservoir and the well results. In the future work, we will experiment fully implicit scheme with all polymer physics derived. The goal is to determine if this scheme provides more accurate results with an attractive calculation time, especially for core flood simulations. In particular, the impact of the implicit resolution of the polymer non linear effect either on the linear solver convergence or on the Newton's algorithm convergence has to be studied carefully.

REFERENCES

1 http://www.fossil.energy.gov/programs/oilgas/eor/index.html.

2 http://www.energy.ca.gov/process/pubs/electrotech_opps_tr113836.pdf.

3 PumaFlow (2013) Reference manual, release V600, Beicip Franlab.

4 Green D.W., Willhite G.P. (1998) Enhanced Oil Recovery, Society of Petroleum Engineers Textbook Series Vol. 6.

5 Lake L. (1989) Enhanced Oil Recovery, Prentice Hall.

6 Peaceman D.W. (1977) Fundamentals of Numerical Reservoir Simulation, Elsevier Science Inc., New York.

7 Bondor P.L., Hirasaki G.J., Tham M.J. (1972) Mathematical Simulation of Polymer Flooding in Complex Reservoirs, *SPE Journal* **12**, 5, 369-382.

8 Han C., Delshad M., Sepehrnoori K., Pope G.A. (2005) Fully Implicit, Parallel, Compositional Chemical Flooding Simulator, *SPE Annual Technical Conference and Exhibition*.

9 John A., Han C., Delshad M., Pope G.A., Sepehrnoori K. (2004) A New Generation Chemical Flooding Simulator, *SPE Paper* 89436, Proceeding of the SPE/DOE Fourteenth Symposuum on Improved Oil Recovery, Tulsa, OK, 17-21 April, *SPE Journal* **10**, 2, 206-216.

10 Trangenstein J.A., Bell J.B. (1989) Mathematical Structure of the Black-Oil Model for Petroleum Reservoir Simulation, *SIAM Journal on Applied Mathematics* **49**, 3, 749-783.

11 Sorbie K.S. (1991) Polymer-improved Oil Recovery, Springer.

12 Preux C., McKee F. (2011) Study and Approximation of IMPES Stability: the CFL Criteria Finite Volumes for Complex Applications VI Problems & Perspectives, Springer, Proceedings in Mathematics **4**, 713-721.

13 Buckley S.E., Leverett M.C. (1941) Mechanism of Fluid Displacement in Sand, *Trans. AIME* **146**, 107-116.

14 Welge H.J. (1952) A Simplified Method for Computing Oil Recovery by Gas or Water Drive, *Petroleum Transactions, AIME* **195**, 91-98.

15 Gratien J.-M., Magras J.-F., Quandalle P., Ricois O. (2004) Introducing a New Generation of Reservoir Simulation Software, 9th European Conference on the Mathematics of Oil Recovery, ECMOR IX, Cannes, 30 Aug.-2 Sept.